CHEMISTRY
A EUROPEAN JOURNAL

DOI: 10.1002/chem.200902455

Amido-3-hydroxypyridin-4-ones as Iron(III) Ligands

Sirivipa Piyamongkol,[c] Yong M. Ma,[a] Xiao L. Kong,[a] Zu D. Liu,[a] Mutlu D. Aytemir,[a] Dick van der Helm,[b] and Robert C. Hider*[a]

Abstract: The synthesis and physicochemical properties of a range of 2- and 6-amido-3-hydroxypyridin-4-ones are described. All the amido-substituted 3-hydroxypyridin-4-ones have lower pK_a values than 1,2-dimethyl-3-hydroxypyridin-4-one (deferiprone). This is due to the inductive effect of the amido group. Furthermore, the pK_a values of the 3-hydroxy group in 1-non-substituted pyridinones are dramatically lower than those of the corresponding 1-alkyl analogues, indicating that a strong hydrogen bond exists between the 2-amido function and the 3-oxygen anion, which stabilises the anion. As a result of the decreased competition with protons, the pFe^{3+} values of this group of molecules are higher than that of deferiprone. The distribution coefficients of these molecules are also increased despite the lack of a hydrophobic 1-alkyl substituent and this is ascribed to the intramolecular hydrogen bond. X-ray diffraction studies confirm the existence of the intramolecular hydrogen bond.

Keywords: acidity · hydrogen bonds · hydroxypyridinones · inductive effects · iron

Introduction

Although iron is an essential element for all living processes, it is toxic when present in excess. In the presence of molecular oxygen, weakly coordinated iron can redox cycle between the two most stable oxidation states, iron(II) and iron(III), thereby generating oxygen-derived free radicals such as the toxic hydroxyl radical.[1,2] Iron overload is observed in haemoglobinopathic disorders such as haemochromatosis, thalassaemia and sickle cell disease. These complications can be relieved by the use of selective iron(III) chelators, which reduce the total body iron load. Desferrioxamine B (DFO; **1**; Scheme 1) is the most widely used iron(III) chelator and has been used for this purpose for over thirty years.[3,4] However, DFO suffers from the disadvantage that it is not orally active and is rapidly cleared by the kidneys.[5,6] Therefore, there is an urgent need to develop an iron(III)-selective, orally active and non-toxic sequestering agent. 3-Hydroxypyridin-4-ones (HPOs) are currently one of the main candidates for the development of such chelators.[7] Indeed, 1,2-dimethyl-3-hydroxypyridin-4-one (deferiprone; **2**; Scheme 1) is one of two orally active iron chelators currently available for clinical use. In an attempt to improve the efficacy of this family of bidentate HPOs, metal selectivity and ligand–metal complex stability are key parameters to be considered.[7,8] The pFe^{3+} value, defined as the negative logarithm of the concentration of the free iron(III) in solution, is a more suitable comparator for molecules of therapeutic potential because it takes into account the effect of ligand basicity, denticity, degree of protonation and difference in metal–ligand stoichiometries, factors which do not influence the corresponding stability constants.[9] Typically, pFe^{3+} values are calculated for $ligand_{[total]} = 10^{-5}$ M, $iron_{[total]} = 10^{-6}$ M and pH 7.4. The pFe^{3+} value of deferiprone is 19.4.[9] To increase the iron-chelating ability further, we have established that introduction of a 1′-hydroxyalkyl group at the 2 position of HPOs leads to an appreciable enhancement of pFe^{3+} values.[10] Chelators with high pFe^{3+} values are predicted not only to be able to scavenge iron efficiently at a lower ligand concentration, but also to dissociate less readily and, therefore, are less likely to redistribute iron to other parts of the body. With 3-hydroxypyridin-4-ones, the increase of the pFe^{3+} value can result from a de-

[a] Dr. Y. M. Ma, Dr. X. L. Kong, Dr. Z. D. Liu, Dr. M. D. Aytemir, Prof. R. C. Hider
Pharmaceutical Science Division, King's College London
150 Stamford Street, London, SE1 9NH (UK)
Fax: (+44) 20-7848-4800
E-mail: robert.hider@kcl.ac.uk

[b] Dr. D. van der Helm
Department of Chemistry and Biochemistry, University of Oklahoma
Norman, Oklahoma (USA)

[c] Dr. S. Piyamongkol
Department of Pharmaceutical Sciences, Faculty of Pharmacy
Chiang Mai University, Chiang Mai, 50200 (Thailand)

Supporting information for this article is available on the WWW under http://dx.doi.org/10.1002/chem.200902455.

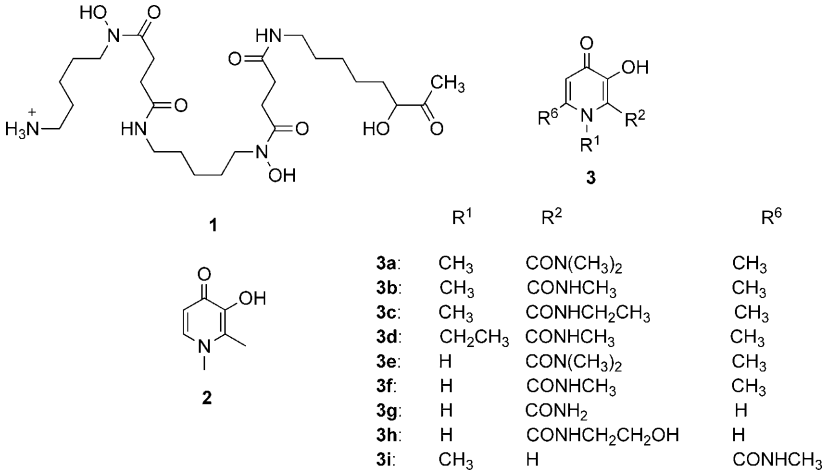

Scheme 1. Structures of DFO (**1**), deferiprone (**2**) and 3-hydroxypyridin-4-one amido derivatives (**3**).

crease of pK_a values corresponding to either of the 3- and 4-pyridinone oxygen atoms.[11,12] These differences may be associated with the enhanced stability of the ionised species. Such enhanced stability can result from a combination of intramolecular hydrogen bonding between the 2-(1′-hydroxyalkyl) group and the adjacent 3-hydroxyl moiety, together with an inductive effect.[10,13] In the present paper, we demonstrate the influence of such factors on the iron-chelating properties of a range of amido HPOs (Scheme 1).

Results and Discussion

The general methodology adopted for the synthesis of 6-methyl-2-amido-3-hydroxypyridin-4-ones is outlined in Scheme 2. Active amide **4** was prepared from 5-hydroxy-2-(hydroxymethyl)-4-pyrone (kojic acid) in several steps as described previously.[13] Active amides were stirred with methylamine or dimethylamine at room temperature to produce the desired 2-amido-substituted pyranones **5a–c**, which were then converted to the corresponding pyridinone derivatives **6a–f** by reaction with an excess of ammonia or an aqueous solution of alkyl amine at 70 °C. The 3-hydroxyl-protected group was hydrogenated to yield the corresponding bidentate ligands **3a–f** as hydrochloride salts.

The synthetic pathway for the 2-amido-3-hydroxypyridin-4-ones is summarised in Scheme 3. Direct conversion of the 2-hydroxymethyl derivative **7**[11] to a carboxylic acid was initially attempted by using Jones reagent.[14] However, this reaction resulted in a poor yield. Thus the primary alcohol **7** was firstly oxidised to the intermediate aldehyde **8** by using $PySO_3$/DMSO (Py = pyridine) before further oxidation to the carboxylic acid **9**. Activation of **9** was achieved prior to reacting with ammonia or ethanolamine. As a result, **10a** and **10b** were obtained in reasonable yields after purification by column chromatography. The benzyl-protected groups were removed by hydrogenation to obtain **3g** and **3h**.

The synthetic route employed for 6-amido-1-methyl-3-hydroxypyridin-4-one is summarised in Scheme 4. The carboxyl pyranone **13** was prepared by directly oxidising 6-hydroxymethyl pyranone **12** by using Jones reagent where the 3-hydroxy group is protected. The reaction proceeded rapidly and in good yield with no indication of oxidative cleavage of the pyran-4-one double bond. Similarly, the acid **13** was activated, coupled with methylamine, converted to the pyridinone, followed by deprotection to yield the final ligand **3i**.

Physicochemical properties of 3-hydroxypyridin-4-ones: All ligands were investigated by spectrophotometric titration. The pH-dependent 2D and 3D UV/Vis spectra of **3b** and **3f** are presented in Figure 1 as examples. An incremental absorption at 278 nm is observed for **3b** with increased pH over the range of pH 1–6 (Figure 1a and b). With continu-

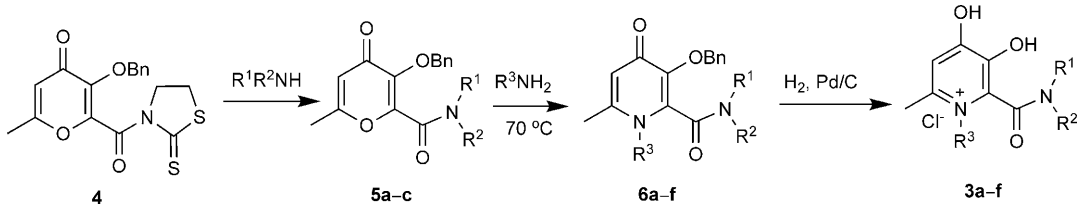

Scheme 2. Synthesis of iron chelators **3a–f** (Bn = benzyl).

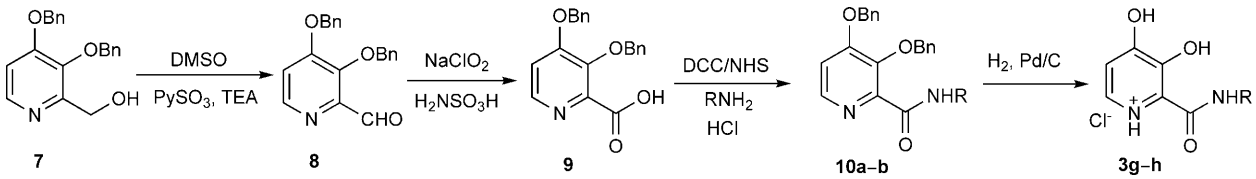

Scheme 3. Synthesis of **3g** and **h**.

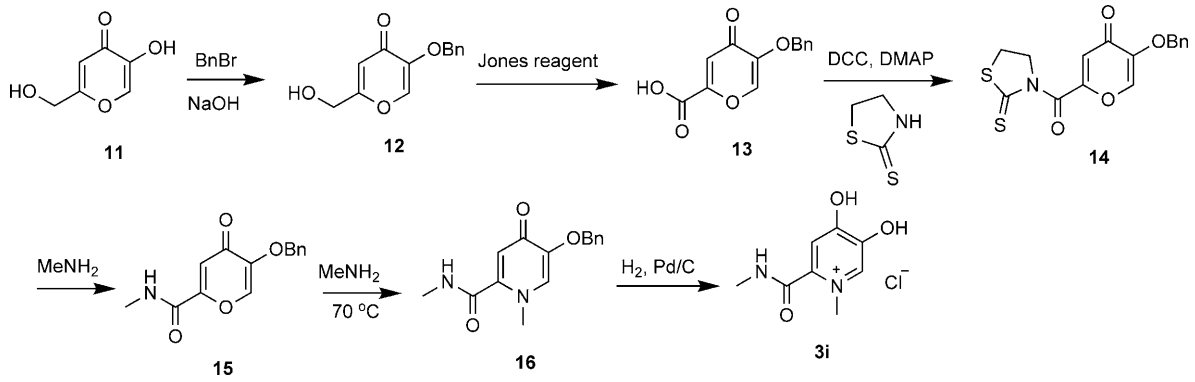

Scheme 4. Synthesis of **3i** from kojic acid.

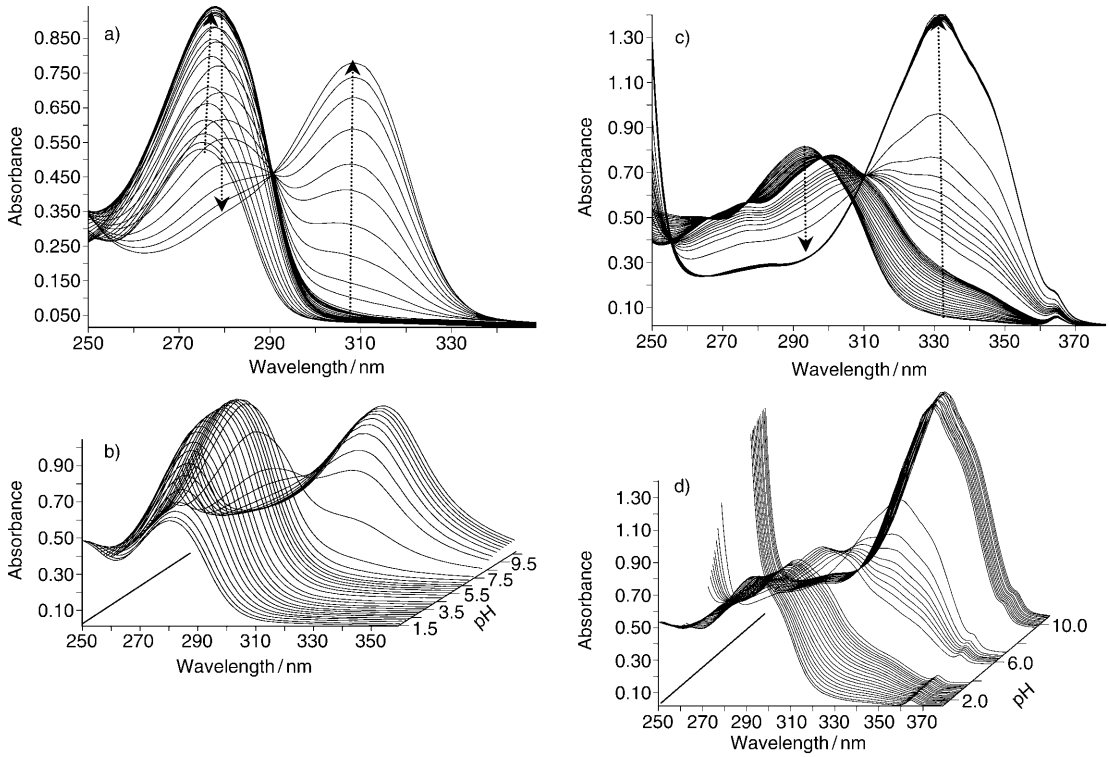

Figure 1. The pH-dependent UV/Vis spectra of **3b** and **3f** over the range pH 1–12: a) 2D spectra of **3b**, b) 3D spectra of **3b**, c) 2D spectra of **3f** and d) 3D spectra of **3f**.

ous increase of pH (pH 6–12), the maximum absorption wavelength is shifted to 315 nm. This phenomenon is similar to that observed in our previous study on **2** and also for other compounds **3a**, **3c–e** and **3i**. The four protonation states of the general 3-hydroxypyridin-4-one structure are shown in Scheme 5. There are two monodeprotonated forms that can exist depending on the location of the labile proton, which can be bound to the oxygen atom of either the 3- or 4-hydroxy group (HB^1 and HB^2). In the previous study centred on **2**, the pK_a value of 3.56 was assigned to the protonation of the 4-oxo group and the pK_a value of 9.64 to the dissociation of the 3-hydroxy group.[15] Because there is a similar pH dependence of the UV/Vis spectra of **2** and **3b**, it is most probable that the 4-hydroxy group of **3b** is first ionised (route 1 of Scheme 5), that is, the pK_a value 2.77 is assigned to the 4-oxo group and the pK_a value 8.44 to the 3-hydroxy group. Route 1 will be favoured by the existence of the two canonical forms of HB^1.

The pH-dependent UV/Vis spectra of **3f** are quite different to those of **2** and **3b** (Figure 1c and d). Over the range pH 2–6, there is one isosbestic point at 298 nm. Over the range pH 6–12, the maximum absorption intensity is increased and shifted to 330 nm with an isosbestic point at 313 nm. A similar phenomenon was also observed for **3g** and **3h**. These distinct differences from **2** and **3b** indicate that the protonation route of **3f** may differ to that of **3b**,

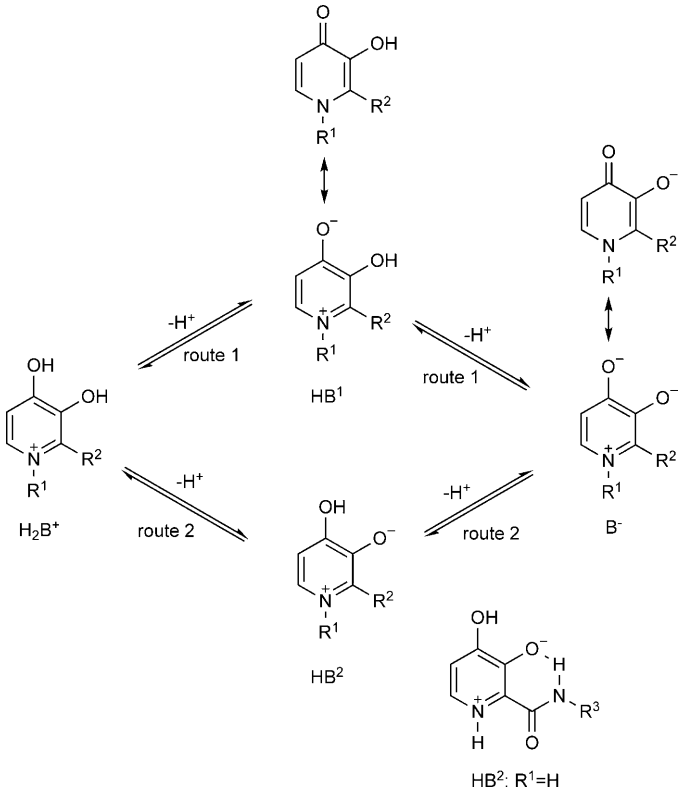

Scheme 5. Ionisation equilibrium of the general 3-hydroxypyridin-4-one.

that is, the 3-hydroxy group may be first ionised to form HB[2] (Scheme 5). A possible driving force for this difference could be the existence of a strong intramolecular hydrogen bond between substituents at the 2 and 3 positions (Scheme 5, $R^1=H$). Thus, the pK_a value of 2.32 is assigned to the 3-hydroxy group and 6.66 to the 4-oxo group.

The physicochemical properties of the entire 3-hydroxypyridin-4-one group are presented in Table 1. All the compounds (**3a–i**) possess lower pK_a values and stability constants for iron(III) than those of **2**, these changes being induced by the introduction of the amido substituent on the ring. Among them, **3a–e** and **3i** have similar pK_a values and the pK_{a2} values fall in the range 8.05–8.45. This group, which relates to the 3-hydroxy substituent, is thought to be ionised after the 4-oxo group through route 1 (Scheme 5). In contrast, **3f–h** have similar pK_a values and the pK_{a2} values fall in the range 1.89–2.32, which relates to the 3-hydroxy group. This group is believed to ionise before the 4-oxo group through route 2. Compounds **3a–h** contain an amido group at the 2 position and **3i** contains an amido group at the 6 position. The presence of an electron-withdrawing amido group leads to the stabilisation of the anions (HB and B^-) and, therefore, to the lower pK_a values. Thus, the introduction of a negative inductive effect plays an important role in reducing the pK_a values of this series of compounds and, therefore, results in an improvement of the associated pFe^{3+} values (Table 1).

In principle, in the group of 1-alkyl-2-amido compounds **3a–d**, compounds **3b–d** could form an intramolecular hydrogen bond between the NH group of the 2-amido group and the ionised 3-hydroxy group. However, there is no such opportunity for **3a** owing to a tertiary amide group located at the 2 position, and yet the pK_a value of the 3-hydroxy group in **3a** was found to be even lower than those of **3b–d**. In an attempt to understand this effect, analogues **3e** and **3i** were synthesised for the physicochemical analysis. Both compounds are structurally incapable of forming an intramolecular hydrogen bond. Again, the pK_a values of the 3-hydroxy group in both are very close to that of **3a**. These combined results suggested that the drop in the pK_{a2} value of compounds **3b–d** results from the inductive effect of the amide substituent and that there is no intramolecular hydrogen bond.

Very interestingly, a further remarkable reduction in the pK_a value of the 3-hydroxy group in **3f** was observed when compared with the **3a–d** group. That is, the pK_a value of the 3-hydroxy group dramatically drops from 8.44 in **3b** or 8.20 in **3e** to 2.32 in **3f**. To expand the study, two analogues **3g** and **3h** were synthesised and both were found to have similar pK_a values to that of **3f**. A marked decrease in the affinity constant for iron(III) ($\log\beta_3$) of **3f** as compared to that of

Table 1. Physicochemical properties of the amido-3-hydroxypyridin-4-ones.

Compound	pK_a (4-oxo, 3-OH)	Affinity constants for Fe^{III}[a] $\log K_1$	$\log K_2$	$\log K_3$	$\log\beta_3$	pFe^{3+}[b]	$D_{7.4}$ (n=5)[c]	F_n[d]	$\log P$[e]
2	3.56, 9.64	14.56	12.19	9.69	36.44	19.4	0.17	0.99	−0.77
3a	2.57, 8.14	12.48	10.81	8.43	31.72	20.0	0.16	0.86	−0.73
3b	2.77, 8.44	13.41	11.47	9.43	34.31	21.7	0.04	0.92	−1.36
3c	2.58, 8.45	12.84	11.88	8.70	33.42	20.9	0.12	0.92	−0.90
3d	2.64, 8.41	12.96	11.27	9.18	33.41	21.0	0.08	0.92	−1.04
3e	2.53, 8.20	12.85	11.18	9.19	33.22	20.4	0.09	0.86	−0.98
3f	6.66, 2.32	14.50	10.49	7.47	32.46	22.8	0.17	0.16	0.03
3g	6.38, 2.19	12.60	10.18	8.28	31.06	21.5	0.01	0.09	−0.91
3h	6.27, 1.89	11.67	10.22	8.53	30.42	20.9	0.15	0.07	0.34
3i	2.32, 8.05	11.77	10.52	8.79	31.08	19.5	0.03	0.83	−1.44

[a] The cumulative affinity constants obtained by summation of the three stepwise equilibrium constants (K_1, K_2, K_3); [b] pFe^{3+} is the negative logarithm of the concentration of the free iron(III) in solution, calculated for $ligand_{[total]}=10^{-5}$ M, $iron_{[total]}=10^{-6}$ M at pH 7.4; [c] $D_{7.4}$ is the distribution coefficient (n-octanol/water) at pH 7.4; [d] F_n is the fraction of non-ionised species calculated at pH 7.4; [e] $\log P$ is the logarithm of the partition coefficient of the neutral species (n-octanol/water).

2 was also found. However, the pFe^{3+} value of **3f** was increased to 22.8. Within the group **3f–h**, in which the pK_a values are similar, the $\log\beta_3$ value decreases from 32.46 to 30.42 and the pFe^{3+} value decreased correspondingly from 22.8 to 20.85 (Table 1). Surprisingly, **3f** was found to be more hydrophobic ($D_{7.4}=0.17$, in which $D_{7.4}$ is the distribution coefficient (n-octanol/water) at pH 7.4) than **3b** ($D_{7.4}=0.04$), whereas in normal circumstances it would be expected to be more hydrophilic owing to the lack of the 1-methyl substituent. These combined findings can best be explained by the existence of a highly stable intramolecular hydrogen bond between the substituents at the 2 and 3 positions (Scheme 5) in **3f–h**. When the pair **3a** and **3b** (N−methyl compounds) are compared with the pair **3e** and **3f** (NH compounds; Table 2), the differences in physicochemical parameters, such as pK_a, pFe^{3+} and $\log P$ values ($\log P$ is the logarithm of the partition coefficient of the neutral species), are less marked in the former pair. Initially, it was not clear why such a similar structural alteration within each pair could lead to such large changes in physicochemical parameters. These results prompted us to undertake X-ray crystal studies to investigate the conformation of both **3b** and **3f**.

The $\log P$ values of the entire group of pyridinones (Table 1) fit with the above proposed hydrogen-bonding schemes. The three pyridinones (**3a**, **3c** and **3d**), which each possess one additional alkyl carbon over that of **3b**, are less hydrophilic than **3b**. In contrast, the $\log P$ value of **3f** is much more hydrophobic than that of **3b** despite **3f** containing one less alkyl function. This is readily explained by the existence of a strong hydrogen bond between the 2-amido and the 3-hydroxy functions in **3f** and the absence of such a bond in **3b**. The existence of strong intramolecular hydrogen bonds reduces the ability of a molecule to form hydrogen bonds with the solvent. The finding that **3e** is more hydrophilic than **3f** is in agreement with this proposal because an analogous intramolecular hydrogen bond between the 2-amido and 3-hydroxyl functions is not possible. The most hydrophobic pyridinone of the series is **3h**, which presumably, in addition to the 2,3-intramolecular hydrogen bond, also possesses an intramolecular hydrogen bond between the 2-amido oxygen and the aliphatic hydroxyl group.

X-ray crystal structures of 3b and 3f: To understand the effect of the structures on their physicochemical properties better, **3b**, **3f** and their hydrochloride salts were investigated by X-ray diffraction. As examples, views of both neutral ligands from the front of the plane of the pyridine molecules are shown in Figure 2. Bond lengths, angles and selected torsion angles of the **3f** and **3b** neutral ligands are presented in Table 3 and Table 4, respectively.

The structure of **3f** in the neutral state clearly demonstrates that the oxygen in the 3 position (O2) is ionised and its bond length with C5 is 1.279 Å, whereas the oxygen in the 4 position (O1) is protonated and its bond length with C4 is 1.336 Å (Table 3). This finding confirms the existence of HB^2 as the monodeprotonated form and confirms the route 2 deprotonation pathway (Scheme 5). Ligand **3f** is almost planar because the torsion angles of any four atoms in the molecule (except H) are close to 0 or 180° (Figure 2a

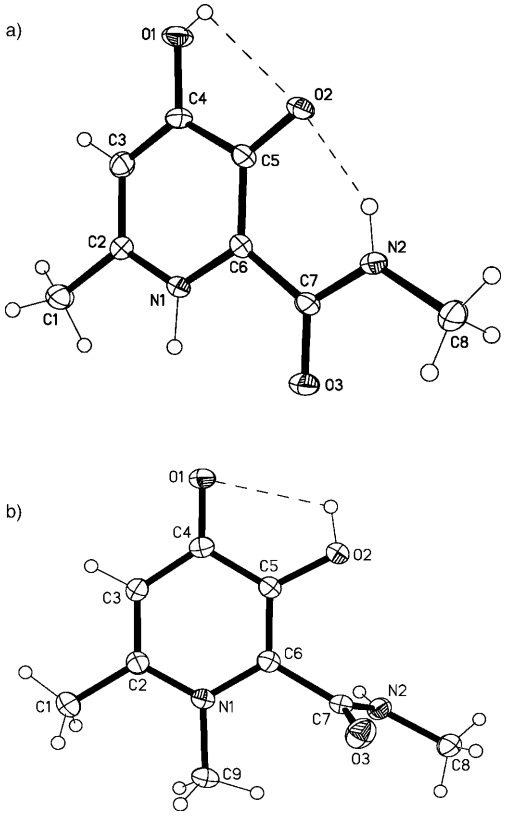

Figure 2. Crystal structures of a) **3f** and b) **3b** viewed from the front of the pyridinone plane.

Table 2. Comparison of the influence of the inductive effect and the hydrogen-bond effect on the pK_a, pFe^{3+} and $\log P$ values.

	3b	**3a**	**3f**	**3e**
	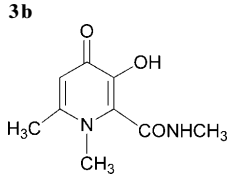	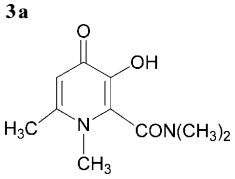	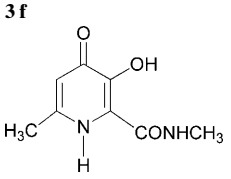	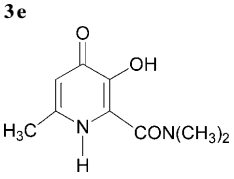
ΔpK_{a1}	0.20		4.13	
ΔpK_{a2}	0.30		−5.88	
ΔpFe^{3+}	1.7		2.4	
$\Delta\log P$	−0.63		1.01	

Table 3. Bond lengths [Å], angles and selected torsion angles [°] of **3f**.

Bond length		Angle		Torsion angle	
O1–C4	1.336 (3)	C2-N1-C6	123.4 (2)	C6-N1-C2-C3	0.3(4)
O2–C5	1.279 (3)	C7-N2-C8	121.4 (2)	C6-N1-C2-C1	−176.4(2)
O3–C7	1.238 (3)	N1-C2-C3	118.7 (2)	N1-C2-C3-C4	−1.0(4)
N1–C2	1.329 (3)	N1-C2-C1	118.3 (2)	C1-C2-C3-C4	175.5(2)
N1–C6	1.365 (3)	C3-C2-C1	122.9 (2)	C2-C3-C4-O1	−179.6(2)
N2–C7	1.328 (3)	C4-C3-C2	120.7 (2)	C2-C3-C4-C5	−0.2(4)
N2–C8	1.449 (3)	O1-C4-C3	119.7 (2)	O1-C4-C5-O2	2.1(4)
C1–C2	1.504 (3)	O1-C4-C5	119.2 (2)	C3-C4-C5-O2	−177.2(2)
C2–C3	1.389 (3)	C3-C4-C5	121.1 (2)	O1-C4-C5-C6	−178.5(2)
C3–C4	1.371 (3)	O2-C5-C6	125.1 (2)	C3-C4-C5-C6	2.1(3)
C4–C5	1.443 (3)	O2-C5-C4	120.0 (2)	C2-N1-C6-C5	1.8(4)
C5–C6	1.410 (3)	C6-C5-C4	114.9 (2)	C2-N1-C6-C7	−178.3(2)
C6–C7	1.481 (3)	N1-C6-C5	121.1 (2)	O2-C5-C6-N1	176.4(2)
O1H–O2	2.339 (3)	N1-C6-C7	114.9 (2)	C4-C5-C6-N1	−2.9(3)
N2H–O2	1.933 (3)	C5-C6-C7	124.0 (2)	O2-C5-C6-C7	−3.4(4)
		O3-C7-N2	123.2 (2)	C4-C5-C6-C7	177.3(2)
		O3-C7-C6	121.3 (2)	C8-N2-C7-O3	−0.2(4)
		N2-C7-C6	115.6 (2)	C8-N2-C7-C6	−179.4(2)
				N1-C6-C7-O3	4.0(3)
				C5-C6-C7-O3	−176.2(2)
				N1-C6-C7-N2	−176.8(2)
				C5-C6-C7-N2	3.1(3)

Table 4. Bond lengths [Å], angles and selected torsion angles [°] of **3b**.

Bond length		Angle		Torsion angle	
O1–C4	1.2731 (14)	C2-N1-C6	119.91 (9)	C6-N1-C2-C3	1.16(16)
O2–C5	1.3483 (14)	C2-N1-C9	120.46 (9)	C9-N1-C2-C3	−177.67(10)
O3–C7	1.2268 (14)	C6-N1-C9	119.62 (9)	C6-N1-C2-C1	−178.42(10)
N1–C2	1.359 (2)	C7-N2-C8	121.68 (10)	C9-N1-C2-C1	2.74(16)
N1-C6	1.374 (2)	N1-C2-C3	119.56 (10)	N1-C2-C3-C4	−0.18(18)
N1–C9	1.4773 (14)	N1-C2-C1	118.99 (10)	C1-C2-C3-C4	179.39(10)
N2–C7	1.330 (2)	C3-C2-C1	121.45 (10)	C2-C3-C4-O1	179.07(11)
N2–C8	1.455 (2)	C4-C3-C2	123.49 (10)	C2-C3-C4-C5	−1.52(17)
C1–C2	1.497 (2)	O1-C4-C3	124.09 (10)	O1-C4-C5-O2	2.20(17)
C2–C3	1.372 (2)	O1-C4-C5	121.31 (10)	C3-C4-C5-O2	−177.23(10)
C3–C4	1.414 (2)	C3-C4-C5	114.59 (10)	O1-C4-C5-C6	−178.24(10)
C4–C5	1.436 (2)	O2-C5-C6	118.37 (10)	C3-C4-C5-C6	2.33(16)
C5–C6	1.367 (2)	O2-C5-C4	121.10 (10)	O2-C5-C6-N1	178.05(10)
C6–C7	1.510 (2)	C6-C5-C4	120.54 (10)	C4-C5-C6-N1	−1.53(17)
O2H–O1	2.358 (2)	N1-C6-C5	121.87 (10)	O2-C5-C6-C7	2.65(16)
		N1-C6-C7	118.25 (9)	C4-C5-C6-C7	−176.92(9)
		C5-C6-C7	119.73 (10)	C2-N1-C6-C5	−0.31(17)
		O3-C7-N2	125.61 (11)	C9-N1-C6-C5	178.54(10)
		O3-C7-C6	119.41 (10)	C2-N1-C6-C7	175.15(9)
		N2-C7-C6	114.98 (10)	C9-N1-C6-C7	−6.00(15)
				C8-N2-C7-O3	−1.58(18)
				C8-N2-C7-C6	178.49(9)
				C5-C6-C7-O3	95.95(14)
				N1-C6-C7-O3	−79.61(14)
				C5-C6-C7-N2	−84.12(13)
				N1-C6-C7-N2	100.32(12)

and Table 3). Thus, the amide substituent on the 2 position is coplanar with the pyridine ring. This structural arrangement results in a N2–O2 bond length of only 2.657 Å, a value that is similar to that reported for *N*,*N*′,*N*″-tris((1,2-didehydro-1-hydroxy-2-thioxopyrid-6-yl)-carbonyl)-2,2′,2″-triaminotriethylamine, 2.62 Å,[16] which is indicative of a very strong hydrogen-bond interaction between the amide NH and the adjacent oxygen atom. Thus, the pK_a values of **3f** are probably influenced by two factors, namely, the presence of an electronegative function at the 2 position and the intramolecular hydrogen bond, which are associated with the uniquely high pFe^{3+} value (Table 1). Interestingly, the extremely efficient intramolecular hydrogen bond in **3f** also reduces its ability to form hydrogen bonds with water molecules, resulting in the surprising hydrophobic properties.

In contrast, the structure of **3b** in the neutral state shows that the oxygen in the 3 position (O2) is protonated and its bond length with C5 is 1.3483 Å, whereas the oxygen in the

4 position (O1) is ionised and forms a double bond with C4 with a length of 1.2731 Å (Figure 2b and Table 4). This finding confirms our conclusion that **3b** is deprotonated through the route 1 pathway. The amide functional group is almost perpendicular to the heterocyclic ring with the torsion angles of C5-C6-C7-O3, N1-C6-C7-O3, C5-C6-C7-N2 and N1-C6-C7-N2 at approximately 90° (Table 4). This is attributed to the steric constraint between the N-methyl group at position 1 and the amide O or NH at the 2 position. The distance between N2–H2 and O2 is 3.24 Å, which is much longer than the sum of van der Waals radii (2.6 Å).[17] Therefore, it is unlikely that a hydrogen bond forms between N2–H2···O2. This finding agrees well with the conclusion obtained from the spectroscopic studies.

In contrast to the two neutral forms of **3b** and **3f**, which show marked differences in structure, the bond lengths in the two corresponding HCl salts are similar although the amide group is only coplanar with the aromatic ring in **3f**.

Iron mobilisation efficacies: The in vivo iron mobilisation abilities of **3a**, **3b** and **3f** were compared with that of **2** in the ^{59}Fe ferritin-labelled rat model (Table 5). All the amide

Table 5. Iron mobilisation efficacy studies of **3a**, **3b** and **3f** in the ^{59}Fe ferritin-loaded rat model. All chelating ligands were given orally at the corresponding dose and control rats were administered with an equivalent volume of water. Values are expressed as means ± SD ($n=5$; SD = standard deviation).

Chelator	$D_{7.4}$	Dose at 450 μmol kg^{-1} % Fe mobilisation	Dose at 300 μmol kg^{-1} % Fe mobilisation	Dose at 150 μmol kg^{-1} % Fe mobilisation
control	–	3.87 ± 1.0	3.87 ± 1.0	3.87 ± 1.0
2	0.17	13.4 ± 5.2	9.2 ± 2.2	6.3 ± 2.1
3a	0.16	35.0 ± 9.8	–	–
3b	0.04	58.7 ± 10.9	54.1 ± 14.1	33.1 ± 6.8
3f	0.17	50.1 ± 9.6	41.4 ± 2.3	25.3 ± 3.4

derivatives were found to be more potent iron(III) scavengers than **2** when given at the dose of 450 μmol kg^{-1}. This is due to their higher pFe values and lower rate of metabolism (unpublished data). Based on the physicochemical characteristics (Table 1), **3f** might have been expected to be superior to **3b** for removing iron in vivo because **3f** is more hydrophobic ($D_{7.4}=0.17$ vs. 0.04) and possesses a higher pFe^{3+} value (22.8 vs. 21.7) than **3b**. However, another limiting factor for chelating ligands is their net charge at physiological pH. Normally only the neutral uncharged form crosses biological membranes at an appreciable rate. With **3b**, over 85% of the total drug is in the non-ionised form (Table 1), enabling **3b** to penetrate membranes readily. In contrast, for **3f**, both pK_a values are below 7.4 and, therefore, it is largely ionised at pH 7.4 and only 16% is present as the zwitterion form (HB^2 in Scheme 5). As a result cell penetration is predicted to be reduced, and this probably contributes to its lower iron-mobilisation efficacy.

Ligand **3f** was also found to be inferior to **3b** in its ability to scavenge iron(III) at all three doses (150, 300 and 450 μmol kg^{-1}; Table 5). At the chelator dose of 150 μmol kg^{-1} both **3b** and **3f** were found to be truly remarkable in removing more iron than **2** at a dose of 450 μmol kg^{-1}, thus confirming that chelators with high pFe^{3+} values have the potential to remove iron(III) more efficiently at lower ligand concentrations.

Conclusion

There are two effects influencing the pFe^{3+} value of 3-hydroxypyridin-4-one chelators, the inductive effect induced from positions 2 and 6 and the intramolecular hydrogen-bond effect centred at position 2 (**3f–h**). Both the 2- and 6-amido derivatives have been demonstrated to possess such properties, which lead to high pFe^{3+} values at pH 7.4. However, X-ray crystal-structure analyses have demonstrated that intramolecular hydrogen-bond formation is not possible for the 2-amido derivatives with an alkyl function at position 1, as with **3b**, because of the bulk associated with the N-alkyl group. Such intramolecular hydrogen-bond formation is only possible when there is a hydrogen atom at position 1, as in **3f**. Thus, **3f** benefits from both effects and the pK_{a2} value is heavily influenced by the presence of the hydrogen bond. The high pFe^{3+} value has an appreciable effect on the speciation plot of the iron(III) as illustrated in Figure 3.

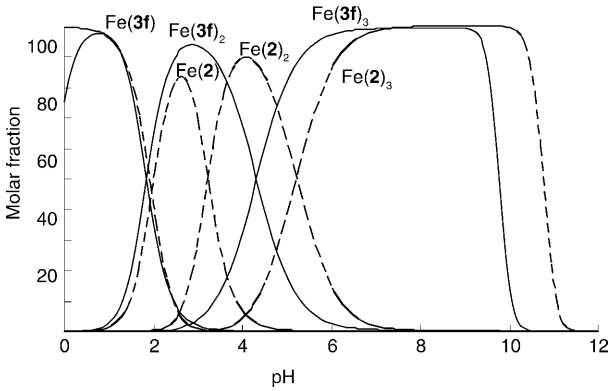

Figure 3. Comparison of the iron complex speciation plots between **3f** (——) and **2** (-----); $[iron]_{total}=10^{-6}$ M and $[ligand]_{total}=10^{-5}$ M.

Under the conditions of the speciation study, **2** begins to dissociate at pH 7.0 and at pH 4.5 the plot is dominated by the 2:1 iron(III) complex. In contrast, the 3:1 iron(III) complex of **3f** does not begin to dissociate until pH 5.5, that is, beyond the pH range experienced within mammalian cells, namely, pH 5.5–8.0. The difference in their pFe^{3+} values indicates that **3f** binds iron(III) 10^3 times more tightly than **2** at pH 7.4. The range of pFe^{3+} values for the corresponding 2-(1′-hydroxyalkyl) series of pyridinones was found to be 20.4–21.5[10] and so none of these compounds were found to bind iron(III) as tightly as **3f**. This information demon-

strates that a high pFe^{3+} value bidentate compound can behave like a hexadentate ligand in that the 3:1 iron(III) complex is strongly favoured.

Despite the high pFe^{3+} value and distribution coefficient values of **3f**, the iron mobilisation efficacy of **3f** was found to be lower than that of **3b**. This is almost certainly a result of the dominant ionised form at pH 7.4. In contrast to **3f**, the excellent ability of **3b** in removing excess iron from the liver demonstrates that it penetrates biological membranes in an efficient manner.

Experimental Section

For synthetic details, analytical data, procedures for the determination of physicochemical properties and in vivo studies, see the Supporting Information.

Acknowledgements

The authors would like to thank Apotex Research Canada for supporting the research project and The Royal Thai Government and the Faculty of Pharmacy, Chiang Mai University, Chiang Mai, Thailand for a studentship to S. Piyamongkol. Also thanks to Dr D. R. Powell for completing the crystallographic results. D. van der Helm acknowledges support from the National Institutes of Health, GM21822.

[1] R. R. Crichton, *Inorganic Biochemistry of Iron Metabolism*, West Sussex, John Wiley & Sons, **2001**.
[2] B. Halliwell, J. M. C. Gutteridge, *Free Radicals in Biology and Medicine*, Oxford, Oxford University, **2007**.
[3] A. V. Hoffbrand, B. Wonke, *Bailliere's Clin. Haematol.* **1989**, *2*, 343–343.
[4] R. Sephton-Smith, *Br. Med. J.* **1962**, *2*, 1577–1580.
[5] M. J. Pippard, *Bailliere's Clin. Anaesthesiol.* **1989**, *3*, 323–343.
[6] M. R. Summers, A. Jacobs, D. Tudway, P. Perera, C. Ricketts, *Br J Haematol* **1979**, *42*, 547–555.
[7] G. S. Tilbrook, R. C. Hider in *Metal Ions in Biological Systems* (Eds.: A. Sigal, H. Sigal), Marcel Dekker, New York, **1998**, pp. 691–730.
[8] R. C. Hider, H. H. Khodr, Z. D. Liu, G. Tilbrook in *Metal Ions in Biology and Medicine* (Eds.: P. Collery, P. Bratter, d. B. V. Negretti, L. Khassanova, J. C. Etienne), John Libbey Eurotext, Paris, **1998**, pp. 51–55.
[9] Z. D. Liu, R. C. Hider, *Med. Res. Rev.* **2002**, *22*, 26–64.
[10] Z. D. Liu, H. H. Khodr, D. Y. Liu, S. L. Lu, R. C. Hider, *J. Med. Chem.* **1999**, *42*, 4814–4823.
[11] S. Piyamongkol, Z. D. Liu, R. C. Hider, *Tetrahedron* **2001**, *57*, 3479–3486.
[12] V. M. Nurchi, T. Pivetta, J. I. Lachowicz, G. Crisponi, *J. Inorg. Biochem.* **2009**, *103*, 227–236.
[13] Z. D. Liu, S. Piyamongkol, D. Y. Liu, H. H. Khodr, S. L. Lu, R. C. Hider, *Bioorg. Med. Chem.* **2001**, *9*, 563–573.
[14] K. Bowden, I. M. Heilbron, E. R. H. Jones, B. C. L. Weedon, *J Chem. Soc* **1946**, 39–45.
[15] P. S. Dobbin, R. C. Hider, A. D. Hall, P. D. Taylor, P. Sarpong, J. B. Porter, G. Y. Xiao, D. Vanderhelm, *J. Med. Chem.* **1993**, *36*, 2448–2458.
[16] K. Abu-Dari, K. N. Raymond, *Inorg. Chem.* **1991**, *30*, 519–524.
[17] A. Bondi, *J. Phys. Chem.* **1964**, *68*, 441–451.

Received: September 4, 2009
Published online: April 15, 2010

